Redox Biology 76 (2024) 103312

Contents lists available at ScienceDirect

Redox Biology

journal homepage: www.elsevier.com/locate/redox

Plin4 exacerbates cadmium-decreased testosterone level via inducing ferroptosis in testicular Leydig cells

Xu-Dong Zhang [a,b,1], Jian Sun [a,b,1], Xin-Mei Zheng [a,b], Jin Zhang [a,b], Lu-Lu Tan [a,b], Long-Long Fan [a,b], Ye-Xin Luo [a,b], Yi-Fan Hu [a,b], Shen-Dong Xu [a,b], Huan Zhou [a,b], Yu-Feng Zhang [a,b], Hao Li [a,b], Zhi Yuan [a,b], Tian Wei [a,b], Hua-Long Zhu [a,b,c], De-Xiang Xu [a,b,c], Yong-Wei Xiong [a,b,c,**], Hua Wang [a,b,c,*]

[a] *Department of Toxicology, School of Public Health, and Center for Big Data and Population Health of IHM, School of Public Health, Anhui Medical University, Hefei 230032, China*

[b] *Key Laboratory of Environmental Toxicology of Anhui Higher Education Institutes, China*

[c] *Key Laboratory of Population Health Across Life Cycle (Anhui Medical University), Ministry of Education of the People's Republic of China, China*

A R T I C L E I N F O

Keywords:
Ferroptosis
m6A modification
Testosterone deficiency
Environment stress
Perilipins
Lipid droplet

A B S T R A C T

Strong evidence indicates that environmental stressors are the risk factors for male testosterone deficiency (TD). However, the mechanisms of environmental stress-induced TD remain unclear. Based on our all-cause male reproductive cohort, we found that serum ferrous iron (Fe^{2+}) levels were elevated in TD donors. Then, we explored the role and mechanism of ferroptosis in environmental stress-reduced testosterone levels through in vivo and in vitro models. Data demonstrated that ferroptosis and lipid droplet deposition were observed in environmental stress-exposed testicular Leydig cells. Pretreatment with ferrostatin-1 (Fer-1), a specific ferroptosis inhibitor, markedly mitigated environmental stress-reduced testosterone levels. Through screening of core genes involved in lipid droplets formation, it was found that environmental stress significantly increased the levels of perilipins 4 (PLIN4) protein and mRNA in testicular Leydig cells. Further experiments showed that *Plin4* siRNA reversed environmental stress-induced lipid droplet deposition and ferroptosis in Leydig cells. Additionally, environmental stress increased the levels of METTL3, METTL14, and total RNA m6A in testicular Leydig cells. Mechanistically, S-adenosylhomocysteine, an inhibitor of METTL3 and METTL14 heterodimer activity, restored the abnormal levels of *Plin4*, Fe^{2+} and testosterone in environmental stress-treated Leydig cells. Collectively, these results suggest that *Plin4* exacerbates environmental stress-decreased testosterone level via inducing ferroptosis in testicular Leydig cells.

1. Introduction

Testosterone deficiency (TD), also known as hypotestosteronemia, is characterized by low serum androgen levels in adult males [1–3]. TD is prevalent and has a high incidence worldwide. In 2004, a North American study found a 38.7 % prevalence of TD among 2162 adult males [4]. Subsequently, the 2010 European Male Aging Study, which assessed over 3000 men aged 40 to 79, reported a TD prevalence of 21.3 % [5]. Most recently, in 2020, a concerning finding was reported in China: among 1472 men aged 40 to 69, the prevalence of TD was 42.76 % [6]. Over the past two decades, TD has persistently impacted the health of adult men worldwide, leading to decreased libido and erectile dysfunction, ultimately resulting in male infertility [7–9]. Multiple population studies have confirmed that many male infertility patients have low or near-low serum testosterone levels [10]. For instance, a longitudinal study from Denmark found a significant negative correlation between semen quality and testosterone levels in male infertility patients [11]. Additionally, a proteomics study on human testosterone

* Corresponding author. Environmental Toxicology Laboratory and Department of Toxicology, School of Public Health, Anhui Medical University, Hefei, 230032, China.

** Corresponding author. Environmental Toxicology Laboratory and Department of Toxicology, School of Public Health, Anhui Medical University, Hefei, 230032, China.

E-mail addresses: xiongyongweidev@126.com (Y.-W. Xiong), wanghuadev@ahmu.edu.cn (H. Wang).

[1] These authors contributed equally to this work.

https://doi.org/10.1016/j.redox.2024.103312
Received 1 August 2024; Received in revised form 13 August 2024; Accepted 13 August 2024
Available online 17 August 2024

deficiency revealed the role of testosterone in regulating sperm protein expression and its importance in male infertility [12]. These findings emphasize the potential importance of restoring normal testosterone levels for the treatment of infertility. In addition, TD was strongly associated with osteoporosis, cardiovascular diseases, and diabetes [13]. Numerous studies indicated that exposure to various stressors, such as smoking, endocrine disruptors, and heavy metals, might trigger TD [14–16]. For instance, a 20-year longitudinal study showed that the decline in testosterone levels in men was closely related to unhealthy lifestyles such as smoking [17]. Additionally, endocrine disruptors like phthalates and bisphenol A affected testosterone levels through mechanisms such as inducing oxidative stress, triggering apoptosis, and inhibiting steroidogenic enzymes [15]. Furthermore, exposure to heavy metals like lead and mercury has been directly linked to testicular dysfunction and reduced testosterone levels [18]. As representative substances of various environmental stressors, increasing evidence showed that cadmium (Cd) was a common environmental stressor inducing TD. Epidemiological studies found a negative correlation between blood Cd levels and serum testosterone levels in adult men [19,20]. Animal experiments further confirmed that Cd inhibited testosterone synthesis in mouse testes [16,21,22]. Nevertheless, the exacted mechanism by which environmental stress induces TD remains unclear.

Ferroptosis is a novel type of programmed cell death associated with intracellular ferrous iron overload and lipid peroxidation [23–25]. In addition, the inactivation of the antioxidant defense system (such as glutathione and GPX4) is also crucial in the process of ferroptosis [26,27]. Ferroptosis was closely associated with various male reproductive diseases, including testicular dysgenesis, spermatogenesis disorders, and blood-testis barrier (BTB) disruption [28–31]. Additionally, environmental stress-induced ferroptosis was gradually discovered in various organs, including Cd-induced ferroptosis in mouse kidneys, livers, and pancreas [32–35]. Most recently, a research study indicated that environmental stress induced oxidative stress and ferroptosis in the testes of pubertal mice, and thereby damaging testicular development and spermatogenesis [31]. Although it is known that environmental stress can trigger ferroptosis, the specific mechanism and its impact on testosterone levels remain unclear.

Lipid droplets are storage organelles at the center of lipid and energy homeostasis, playing an important role in lipid homeostasis regulation and testicular spermatogenesis [36–38]. With the increasing attention on ferroptosis, the relationship between lipid droplets and ferroptosis needs further exploration urgently. A recent study indicated that lipid droplet deposition promoted lipid peroxidation, and thereby initiated ferroptosis in mouse livers [39]. It's well known that lipid droplets are mainly regulated by perilipins family members (*Plin1-5*), which are crucial for the formation, stabilization, and metabolism of lipid droplets [40,41]. Previous studies showed that perilipins participated in the accumulation of lipid droplets in stromal vascular cells, liver cells and neurons [42–45]. These studies consistently indicated that perilipins may have a potential role in regulating lipid droplet deposition and triggering ferroptosis. However, no studies have yet explored the impact of perilipin-regulated lipid droplets on environmental stress-induced ferroptosis in testes.

In the present study, our primary aim was to explore the relationship between TD and Fe^{2+} levels based on our all-cause male reproductive cohort. Next, we investigated the role of ferroptosis in environmental stress-reduced testosterone levels by using ferrostatin-1 (Fer-1), a specific ferroptosis inhibitor, in a mouse intervention study. Subsequently, *Plin4* siRNA intervention was used to observe the effect of *Plin4* upregulation on environmental stress-induced ferroptosis in TM3 cells. Finally, S-adenosylhomocysteine (SAH, a m6A modification inhibitor) was utilized to investigate the role of m6A modification in environmental stress-induced upregulation of *Plin4* in TM3 cells.

2. Materials and approaches

2.1. Reagents

Cadmium chloride ($CdCl_2$, 202908) was obtained from Sigma Chemical Co (St. Louis, MO). Ferrostatin-1 (Fer-1, HY-100579) and S-adenosylhomocysteine (SAH, HY-19528) sourced from MedChemExpress (New Jersey, United States). Antibodies for steroidogenic acute regulatory protein (StAR, 8449S), methyltransferase 14 (METTL14, 51104S) and beta-actin (β-Actin, 4970S) were obtained from Cell Signaling Technology (Beverley, MA). Antibodies against Glutathione Peroxidase 4 (GPX4, ab125066) and METTL3 (ab195352) were sourced from Abcam (Cambridge, MA, USA). Antibody for 4-hydroxynonenal (4-HNE, AB_2735095) obtained from Thermo Fisher Scientific (Shanghai, China). Antibody against perilipin-4 (PLIN4, 55404-1-AP) obtained from Proteintech (Wuhan, China). EpiQuickTM RNA Methylation Quantification Kit was from Epigentek Group Inc (Farmingdale, NY). The Total Iron Colorimetric Assay Kit (E-BC-K772-M) and Ferrous Iron Colorimetric Assay Kit (E-BC-K773-M) were sourced from Elabscience (Wuhan, China). Testosterone ELISA kit (CEA458Ge) manufactured by Cloud-Clone Corp (Wuhan, China). Mouse *Plin4* short interfering RNA was from GenePharma (Shanghai, China).

2.2. All-cause reproductive cohort study

To investigate the causes of male testosterone deficiency, an all-cause male reproductive cohort was established. With the informed consent of donors, human whole blood samples (n = 310) were sourced from the Reproductive Medicine Center of the First Affiliated Hospital of Anhui Medical University. Serum was collected by centrifuging whole blood samples at 3000 g for 15 min at 4 °C. Based on serum testosterone levels of 300 ng/dL (10.4 nmol/L), donors were divided into groups with normal testosterone levels and groups with testosterone deficiency. Throughout its execution, the study design adhered to the regulations regarding human research donors. This study received ethical approval from the Clinical Research Ethics Committee of the First Affiliated Hospital of Anhui Medical University (Approval No: PJ2023-04-12).

2.3. Animal experiment

All procedures involving animals were conducted in strict adherence to the humane treatment standards set forth by the Laboratory Animal Science Association at Anhui Medical University (ethical approval number LLSC20190297). C57BL/6J mice were supplied by Beijing Vital River Laboratory Animal Technology Co., Ltd (Beijing, China). All mice were freely fed and watered, and acclimatized for one week under standard conditions (temperature: 20–25 °C, humidity: 50–60 %, 12-h light/dark cycles). $CdCl_2$ was dissolved in saline to create a working solution at 0.1 mg/mL. Fer-1 was dissolved in dimethyl sulfoxide (DMSO) to form a stock solution (10 mg/mL), which was then diluted to a working solution using saline and 20 % sulfobutylether-β-cyclodextrin (SBE-β-CD). The final concentration of DMSO in the working solution did not exceed 0.1 %. The control injection solution was composed of saline mixed with equal parts DMSO and SBE-β-CD.

Experiment 1: The experimental design was utilized to explore the causes and mechanisms underlying the decline in testosterone levels induced by environmental stress (Fig. 2A). Briefly, all male mice were intraperitoneally injected with 1 mg/kg $CdCl_2$ or saline once daily for three days, and then their serum and testes were collected. In this study, the Cd dosage was chosen based on internal exposure levels obtained from population studies and previous research findings [46,47].

Experiment 2: To clarify the role of ferroptosis in environmental stress-decreased testosterone levels, Fer-1, a specific ferroptosis inhibitor, was utilized before the environmental stressor treatment in mice. All male mice were intraperitoneally injected with 2 mg/kg Fer-1, and 30 min later, 1 mg/kg $CdCl_2$ was injected once daily for three days.

Euthanasia was performed 24 h later, and mouse serum and testes were collected.

2.4. Cell culture and treatment

TM3 cells, a cell line derived from mouse testicular Leydig cells, are cultured in DMEM/F-12 medium supplemented with 5 % horse serum, 2.5 % fetal bovine serum, and 1 % penicillin/streptomycin. All cells are maintained in an incubator at 37 °C with 5 % CO_2. To investigate whether environmental stress induces ferroptosis and reduces testosterone levels, cells were treated with $CdCl_2$ (20 μM) for 0, 2, 8, and 24 h. The Cd dosage was based on a prior study [16]. To investigate whether environmental stress induces ferroptosis by elevating *Plin4*-mediated lipid droplet deposition, cells were incubated with *Plin4* siRNA for 24 h, followed by treatment with $CdCl_2$ (20 μM) for 24 h. To investigate the impact of m6A modification on the upregulation of *Plin4* and ferroptosis induced by environmental stress, cells were co-cultured with SAH (10 μM) and $CdCl_2$ (20 μM) for 24 h.

2.5. Measurement of metal elements in human urine

Inductively coupled plasma mass spectrometry (ICP-MS) was used to measure the metal content in urine. Sample pretreatment steps included dilution with 5 % Triton solution and nitric acid to meet the requirements of ICP-MS analysis. The specific procedure was as follows: take 200 μl of urine sample, add 60 μl of 10 ppm gold (Au) internal standard solution, and an appropriate amount of Solution 1 (composed of nitric acid, 5 % Triton, and deionized water), and perform a 30-fold dilution. The treated samples were then analyzed using ICP-MS, with internal standard addition, instrument bias correction, and standard curve establishment, ultimately calculating the metal content in the urine of the population.

2.6. Cell viability assay

According to the instructions for the CCK-8 assay kit (Catalog No: HY-K0301, New Jersey, USA), first, seed an appropriate number of cells in a 96-well plate, and set time points at 0 h, 2 h, 8 h, and 24 h. When cell confluence reaches 60 %, treat the cells with different concentrations of $CdCl_2$ (0 μM, 2.5 μM, 5 μM, 10 μM, 20 μM, 40 μM). At the designated time points, add 10 μl of CCK-8 reagent to each well and incubate at 37 °C, 5 % CO_2 for 1h. Finally, measure the absorbance (OD value) of each well at a wavelength of 450 nm using a microplate reader to assess cell proliferation and viability.

2.7. RNA interference

RNA interference experiments were conducted in accordance with our previous research methods [48]. Briefly, TM3 cells were transfected with a mixture of *Plin4*-specific small interfering RNA (siR) and Lipofectamine 3000. The nucleotide sequence of the *Plin4* siR was 5′-GGCUGGGUGAUAUCUUUCATT-3′ (forward) and 5′-UGAAAGAU AUCACCCAGCCTT-3′ (reverse).

2.8. Biochemical measurement

Above all, whole blood samples from humans and mice were collected, and serum samples were obtained by centrifuging at 3000g for 15 min at 4 °C. Next, a biochemical analyzer measured the levels of triglycerides (TG), total cholesterol (TC), low-density lipoprotein (LDL-C), and high-density lipoprotein (HDL-C). The levels of glutathione (GSH) in mouse testes were measured using commercial kits from Beyotime (Shanghai, China).

2.9. Enzyme-linked immunosorbent assay (ELISA)

According to the instructions provided by Cloud-Clone Corp (Wuhan, China) for the testosterone assay kit, first set up the standard wells, sample wells, and blank wells. Add 50 μl of the sample and working solution A to each well, incubate at 37 °C for 1 h, then wash the plate 3 times. Add working solution B and incubate for another 30 min. Next, wash the plate 5 times, add the substrate solution, incubate at 37 °C for 10 min in the dark, then add the stop solution and measure the absorbance of each well using a microplate reader.

2.10. Malondialdehyde (MDA) measurement

According to the instructions provided by Beyotime (Shanghai, China) for the malondialdehyde (MDA) assay kit, the experimental steps are as follows: First, take 50 mg of fresh testicular tissue and add 500 μl of pre-cooled saline to prepare the tissue homogenate. Then, centrifuge the homogenate at 10000g–12000g, and collect the supernatant. Next, add the test reagent in proportion, mix well, and heat at 100 °C for 15 min. After cooling, centrifuge again, collect the supernatant, and measure the absorbance with a microplate reader to calculate the MDA content.

2.11. Detection of ferrous iron (Fe^{2+})

To begin with, collect whole blood samples from humans and mice, and centrifuge them at 3000g for 15 min at 4 °C to prepare serum samples. According to the instructions provided in the Ferrous Iron Colorimetric Assay Kit by Elabscience (Wuhan, China), proceed as follows. Prepare a standard curve with appropriate concentrations and mix the serum samples with buffer solution. Add standard samples and test samples sequentially to a 96-well plate, then add the coloring solution and mix well. Incubate the plate at 37 °C for 10 min. Finally, measure the OD value of each well at a wavelength of 593 nm using a microplate reader and calculate the ferrous iron content in the serum according to the formula.

2.12. Transmission electron microscopy (TEM)

After removing the fresh testes, 20 μl of 1 % glutaraldehyde fixative was injected using a microsyringe. Then the testes were cut into small pieces (1 mm^3) and fixed in 1 % glutaraldehyde. The samples were dehydrated through a graded ethanol series (50 %, 70 %, 90 %, 100 %) and embedded in EPON 812 resin. Ultrathin sections (70–100 nm) were prepared using Leica EM UC7 (Leica, Germany). After lead citrate staining, imaging was performed using the Thermoscientific Talos L120C G2 (Thermo Fisher, USA).

2.13. Hematoxylin and eosin (H&E) staining

After deparaffinization and hydration, testicular paraffin sections were stained with hematoxylin and eosin. Subsequently, the sections were dehydrated with increasing concentrations of ethanol and cleared in xylene. Finally, the number of nuclei in testicular Leydig cells was quantified with Image J software.

2.14. Oil red O staining experiment

The 5 μm frozen sections of testicular tissue were washed in PBS three times for 3 min each. Next, the sections were immersed in 60 % isopropanol for 2 min and then stained with freshly prepared Oil Red O solution for 10 min. After staining, to eliminate non-specific attachments, the sections were sequentially washed with 60 % isopropanol and PBS, and then stained with hematoxylin. The areas of lipid droplets in testicular Leydig cells were assessed using Image J software, analyzing four testes per group [49].

2.15. Detection of lipid droplets using BODIPY staining

To begin with, the live cells were rinsed twice using PBS solution. Next, freshly prepared BODIPY 493/503 solution (MED25592) was added to the cells and incubated at 37 °C for 20 min for staining. Afterward, the cells were washed again with PBS and counterstained with Hoechst 33342 dye for 6 min. Finally, the cells were observed and imaged using a laser confocal microscope.

2.16. FerroOrange staining

Initially, TM3 cells treated with environmental stress for 24 h were washed with PBS, then Hoechst 33342 dye was added and incubated at 37 °C for 6 min to label the nuclei. After washing the cells again with PBS, 1 μmol/L FerroOrange staining solution was added to each well, and the cells were incubated at 37 °C in a 5 % CO_2 incubator for 30 min. After incubation, the cells were directly observed using a confocal laser scanning microscope.

2.17. Detection of oxidized lipids using C11-BODIPY

As per the manufacturer's instructions, used C11-BODIPY (Thermo Fisher Scientific, Shanghai, China) to detect lipid peroxidation levels in cells. In short, added freshly prepared 10 μM C11-BODIPY solution to the cells and incubated at 37 °C for 30 min. Subsequently, observed oxidized lipids at a wavelength of 510 nm and reduced lipids at a wavelength of 590 nm using a laser confocal microscope.

2.18. Immunoblotting

For detailed reagent and material preparation, please refer to the previously published articles [50,51]. Briefly, total protein was extracted from mouse testes and TM3 cells. The protein extracts were then separated by SDS-PAGE and transferred to PVDF membranes. Following the blocking with 5 % milk, the membranes were incubated with the respective primary and secondary antibodies. Finally, protein expression was detected using a digital imaging system (ChemiDoc™ MP, BIO-RAD, USA). In this study, the concentrations of the primary antibodies for the primary target proteins are listed as follows: GPX4 (1:1000), 4-HNE (1:1000), StAR (1:1000), 3β-HSD (1:1000), PLIN4 (1:1000), METTL3 (1:1000), and METTL14 (1:1000).

2.19. Immunohistochemistry

Testicular sections were dewaxed, rehydrated, quenched for endogenous peroxidase activity, and subjected to antigen retrieval. The sections were incubated overnight with antibody 4-HNE (1:200) at 4 °C. The following day, the sections were treated with a secondary antibody, followed by SP (streptavidin-peroxidase) reaction, DAB (diaminobenzidine) chromogenic reaction, and hematoxylin staining. Ultimately, the area positive for 4-HNE was quantified in the testes.

2.20. Immunofluorescence

The specific experimental protocol referred to previous studies [52]. The key steps of the experiment are outlined as follows: The testicular tissues were dehydrated with a 30 % sucrose solution and then made into 5 μm frozen sections. TM3 cells were cultured on slides and subsequently fixed with 4 % paraformaldehyde for 15 min after exposure to the environmental stressor. To inhibit non-specific binding, the sections were incubated in PBS working solution containing 10 % goat serum for 1.5 h. Afterward, the sections were incubated with the primary antibody (1:200) at 37 °C for 1.5 h, followed by incubation with the fluorescein-conjugated secondary antibody working solution for 1.5 h. The nuclei were stained with DAPI or Hoechst 33342 for 6 min. Finally, the sections were observed using a confocal microscope (Leica THUNDER DMi8).

2.21. Extraction of total RNA and real-time RT-PCR

Total RNAs of testes and cells were extracted with TRIzol reagent (Invitrogen). cDNA was synthesized from total RNAs utilizing the Transcriptor First Strand cDNA Synthesis Kit (Roche, 04897030001). Then the expression of the target gene was detected using the LightCycler® 480 real-time fluorescence quantitative PCR machine (Roche, Switzerland). 18S rRNA served as the internal control. Primers for the target genes are listed in Supplementary Table 1. The expression of target mRNA was analyzed by comparative the CT method.

2.22. Detection of total m6A levels

Total RNA from TM3 cells was isolated using TRIzol reagent. Subsequently, the total m6A levels were measured using the EpiQuickTM RNA Methylation Quantification Kit (Epigentek, USA) following the manufacturer's guidelines.

2.23. Statistical analysis

All data were presented as *mean* ± *S.E.M.* and analyzed using GraphPad Prism 9.0 software. Mean comparisons between the two groups were performed using two-tailed Student's t-test. One-way ANOVA was used to compare means in multiple groups, followed by Šidák post-hoc test to assess significant differences between groups. *P*-value of less than 0.05 was considered statistically significant.

3. Results

3.1. The association between elevated serum ferrous iron (Fe^{2+}) levels and all-cause testosterone deficiency

Among the 317 donors who provided blood samples, 7 adults were excluded due to age mismatch, and 310 donors were successfully included in the study (Fig. 1A). To investigate the reasons for adult testosterone deficiency, the Spearman correlation indicated a negative association of testosterone levels with ferrous iron (Fe^{2+}) and triglyceride (TG) levels, and a strong positive association between Fe^{2+} and TG levels (Fig. 1B). There was no significant age difference between the two groups of donors (Fig. 1C). Donors were divided into normal testosterone levels group and testosterone deficiency group based on a serum testosterone level of 300 ng/dL (10.4 nmol/L). Relative to the control group, the testosterone deficiency group exhibited significantly reduced serum testosterone levels (Fig. 1D). Significant increase in serum Fe^{2+}, TG, and HDL cholesterol (HDL-C) levels was observed among testosterone deficiency participants (Fig. 1E–G). There were no significant differences between the two groups in serum low-density lipoprotein cholesterol (LDL-C), total cholesterol (TC), and urine iron content (Fig. 1H–J). Compared to the healthy control group, Cd levels in the urine of testosterone deficiency donors were significantly elevated (Fig. 1K). Additionally, Spearman correlation analysis showed a negative correlation between Cd levels in urine and testosterone levels (Fig. S1G). As mentioned above, elevated serum Fe^{2+} and TG levels are negatively correlated with testosterone deficiency.

3.2. Environmental stress suppresses testosterone synthesis in mouse testicular Leydig cells

Cadmium (Cd), a typical environmental stressor, is utilized for establishing models of testosterone deficiency in vivo (Fig. 2A). Male mice underwent continuous exposure to environmental stress for three days. Environmental stress didn't affect the body weight and testicular coefficient in male mice, but significantly reduced their serum testosterone levels (Fig. 2B–D). Correspondingly, environmental stress

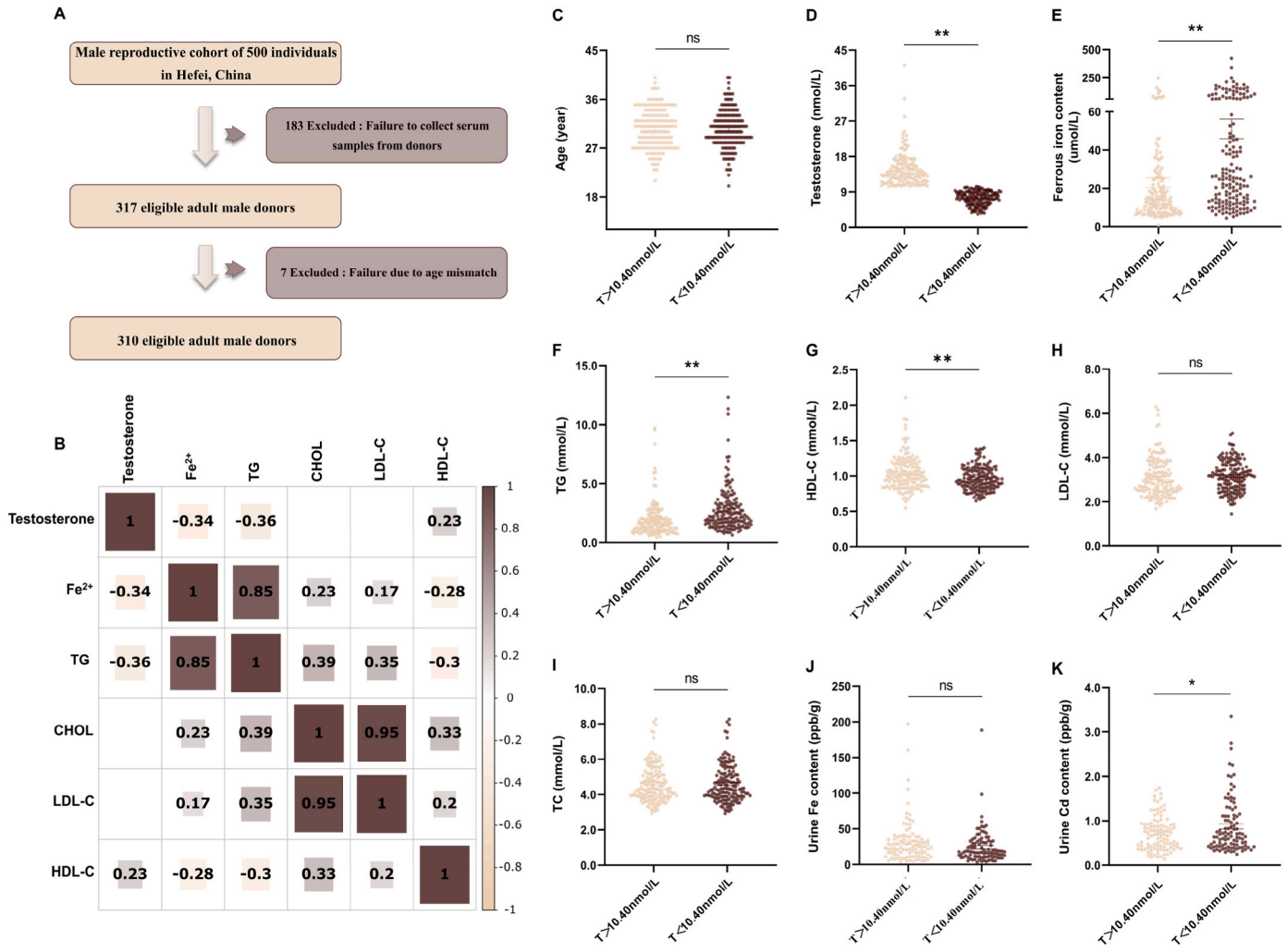

Fig. 1. The association between elevated serum ferrous iron (Fe^{2+}) and all-cause testosterone deficiency. (A–I) Serum was collected from 310 men aged 20–40 years. (A) Flowchart of the study population. (B) Visual representation of Spearman correlations among various indices and correlation strength indicated by the color depth and rectangle size. A blank grid denotes a *P*-value of more than 0.05. (C) Male age. (D) Adult males were divided into two groups based on serum testosterone (T) levels: normal testosterone group (T > 10.4 nmol/L) and testosterone deficiency group (T < 10.4 nmol/L). (E) Ferrous iron (Fe^{2+}). $t = 4.942$, $P < 0.0001$. (F) Triglycerides (TG). $t = 4.371$, $P < 0.0001$. (G) HDL cholesterol (HDL-C). $t = 3.260$, $P = 0.0012$. (G and H) LDL cholesterol (LDL-C) and total cholesterol (TC) levels ($P > 0.05$). (J and K) Urine was collected from 200 men aged 20–40 years. (J) urine Fe levels. ($P > 0.05$). (K) Urine Cd content. $t = 2.262$, $P = 0.0248$. N = 317 for human serum samples and N = 200 for human urine samples. $^{*}P < 0.05$, $^{**}P < 0.01$ and ns $P > 0.05$. (For interpretation of the references to color in this figure legend, the reader is referred to the Web version of this article.)

downregulated the expression of testicular StAR and 3β-HSD, the two testosterone synthesis enzymes (Fig. 2E–G). We further confirmed StAR, primarily located in testicular Leydig cells, was significantly reduced upon environmental stress (Fig. 2H and I). TM3 cells, which are a mouse Leydig cell line, were continuously exposed to environmental stress conditions from 0 to 24 h (Fig. 2J). Environmental stress also led to a reduction in testosterone concentration in the cell medium and lowered the protein level of StAR and 3β-HSD in mouse testicular Leydig cells (Fig. 2K–M). As above, environmental stress significantly inhibits testosterone synthesis in mouse testicular Leydig cells.

3.3. *Environmental stress induces ferroptosis in mouse testicular Leydig cells*

To investigate whether environmental stress induces ferroptosis in testicular Leydig cells, the morphology and tissue structure of mouse testicular Leydig cells were observed. H&E staining results showed that environmental stress reduced the number of Leydig cells in mouse testes (Fig. 3A and B). Subsequently, the ultrastructure of mouse testicular cells was observed under transmission electron microscope (TEM). As presented in Fig. 3C and D, environmental stress lowered the mitochondrial cristae and mitochondrial area in mouse testicular Leydig cells. The accumulation of ferrous iron and lipid peroxides were essential for the execution of ferroptosis. Environmental stress significantly increased serum ferrous iron levels in male mice (Fig. 3E and F). Correspondingly, environmental stress significantly increased malondialdehyde (MDA, a lipid peroxidation marker) levels and decreased glutathione (GSH) levels in mouse testes (Fig. 3G and H). Furthermore, environmental stress markedly reduced GPX4 protein levels and elevated 4-HNE protein levels in mouse testes (Fig. 3I–K). According to immunofluorescent results, environmental stress noticeably downregulated the expression of GPX4 in testicular Leydig cells (Fig. 3L and M). Additionally, lipid peroxidation levels were further measured in TM3 cells. As expected, environmental stress increased levels of oxidative lipids in TM3 cells (Fig. 3N and O). Finally, environmental stress markedly reduced GPX4 protein levels and elevated 4-HNE protein levels in TM3 cells (Fig. 3P–R). As described above, environmental stress triggers ferroptosis in mouse testicular Leydig cells.

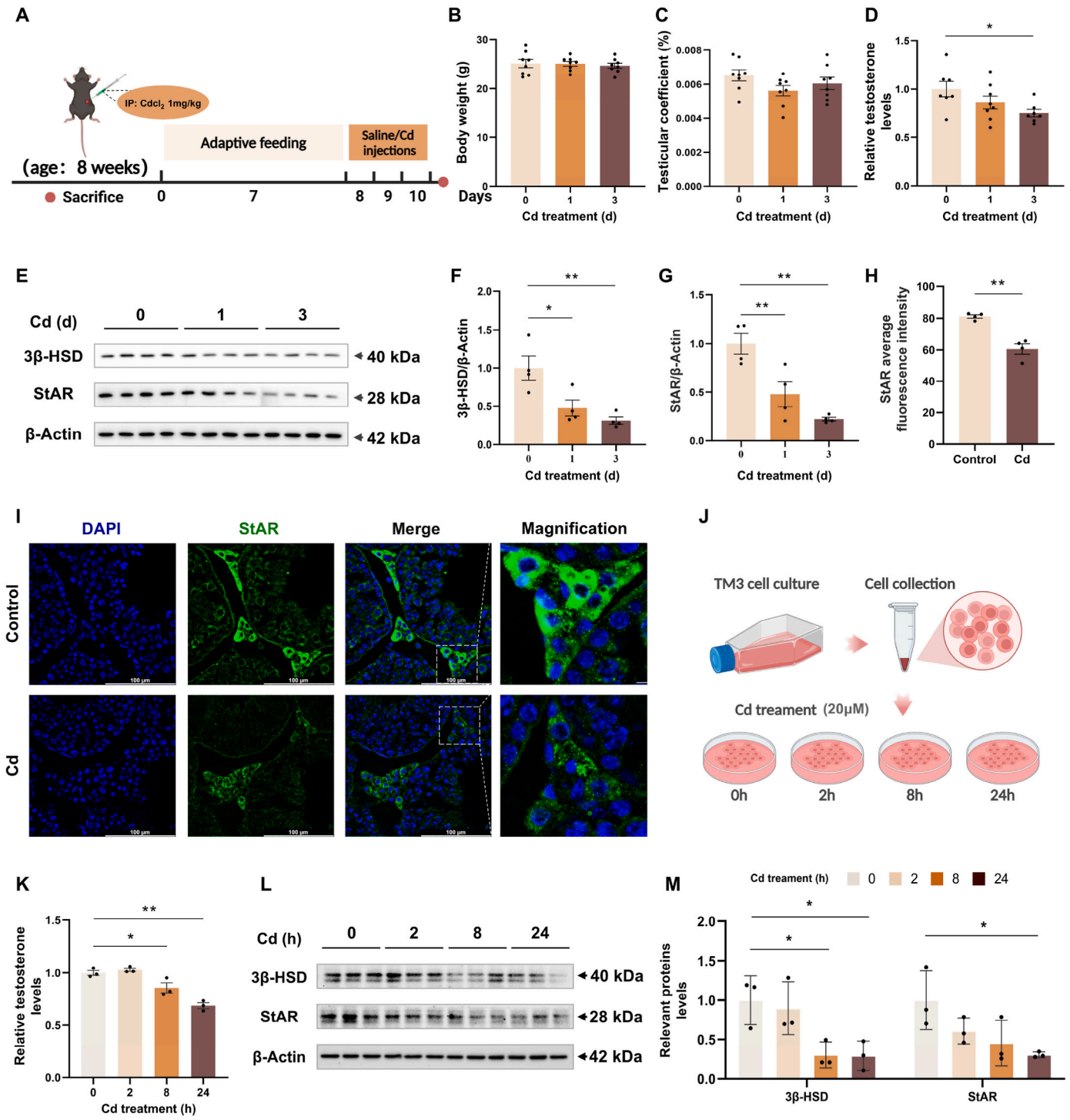

Fig. 2. Environmental stress suppresses testosterone synthesis in mouse testicular Leydig cells. (A–I) Male mice received an intraperitoneal injection of 1 mg/kg $CdCl_2$ daily for three days. Mouse sera and testes were collected. (A) Diagram illustrating the experimental design for the animal experiment. (B) Mouse body weight. (C) Testicular coefficient. (D) Testosterone level in serum. (E–G) The protein expression levels of 3β-HSD and StAR were assessed using immunoblotting in mouse testes. (H and I) Representative images and quantitative results of immunofluorescence staining for StAR, with DAPI highlights the nuclei. Scale bar: 100 μm. (J–M) Mouse testicular Leydig cells (TM3) were exposed to $CdCl_2$ (20 μM) for 0–24 h. (J) Flowchart of TM3 cell culture and $CdCl_2$ treatment. (K) Testosterone levels in cell media. (L and M) The protein expression levels of 3β-HSD and StAR were assessed using immunoblotting in TM3 cells. Data are presented as *mean* ± *S.E.M.* (n = 3–8 per group). $^{*}P < 0.05$, $^{**}P < 0.01$.

3.4. Environmental stress reduces testosterone levels by inducing ferroptosis in mouse testicular Leydig cells

To elucidate the effect of ferroptosis on testosterone levels in testicular Leydig cells, ferrostatin-1 (Fer-1, a specific ferroptosis inhibitor) was used prior to environmental stress in mice. TEM results showed that pre-treatment with Fer-1 effectively inhibited the characteristic morphological changes of ferroptosis induced by the environmental stressor (Fig. 4A and B). Similarly, Fer-1 reversed the depletion of GSH and the accumulation of MDA in environmental stress-exposed

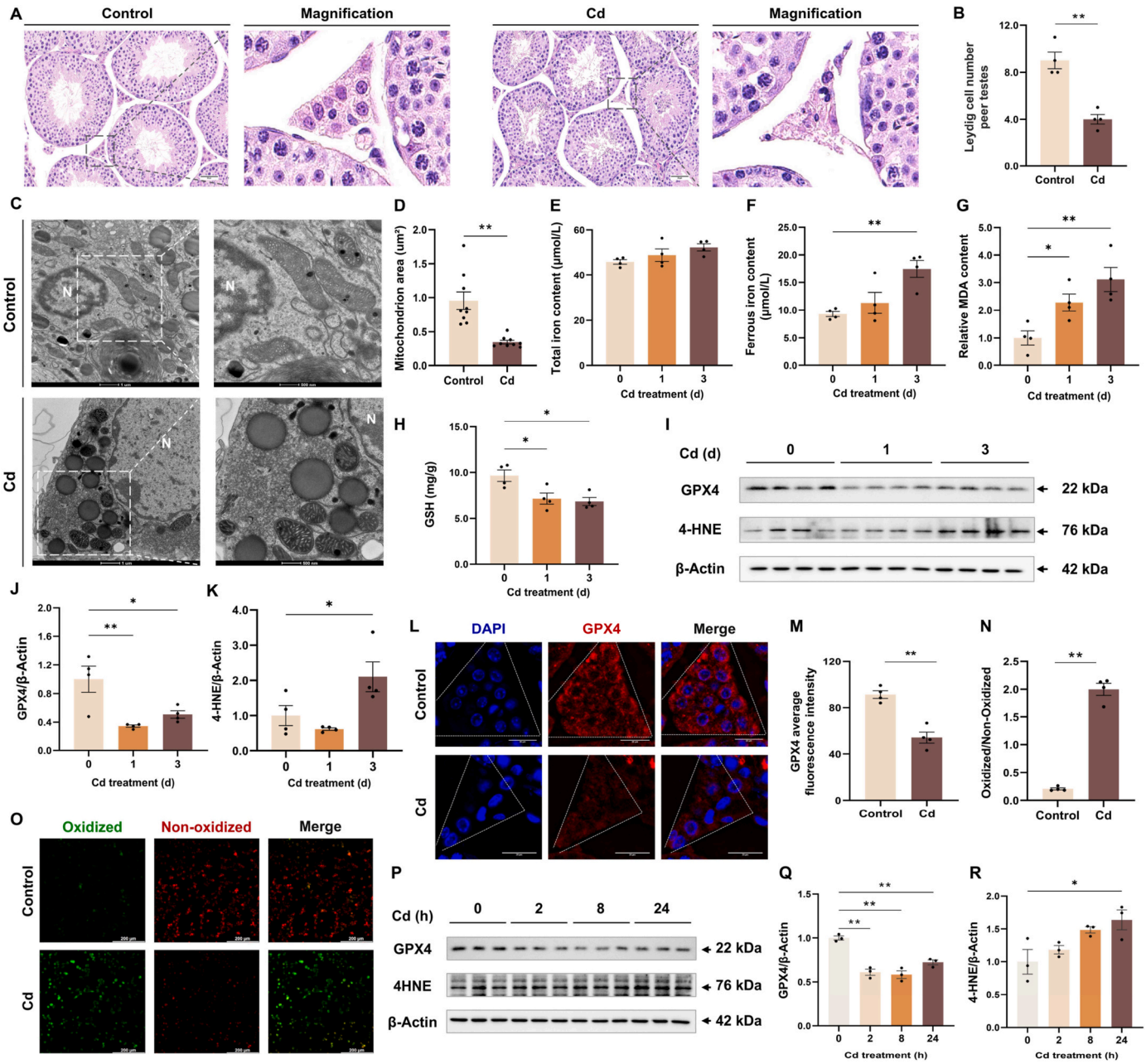

Fig. 3. Environmental stress induces ferroptosis in mouse testicular Leydig cells. (A–M) Male mice received an intraperitoneal injection of 1 mg/kg $CdCl_2$ daily for three days. Mouse sera and testes were collected. (A) Representative H&E staining images and their magnified versions of testes. (B) Quantitative analysis of nuclei in mouse testicular Leydig cells. (C) Representative transmission electron microscopy (TEM) images and their magnified versions in mouse testicular Leydig cells. (D) Mitochondrial area for TEM images. (E) Total iron content in sera. (F) Ferrous iron content in sera. (G) Malondialdehyde (MDA) content in testes. (H) Glutathione (GSH) content in testes. (I–K) The protein expression levels of GPX4 and 4-HNE were evaluated using immunoblotting in mouse testes. (L and M) Representative images and quantitative results of immunofluorescence staining for GPX4, with DAPI marking the nuclei. Scale bar: 20 μm. (N–R) Mouse testicular Leydig cells (TM3) were exposed to $CdCl_2$ (20 μM) for 0–24 h. (N and O) Exemplary images and quantitative results of C11-BODIPY staining for the detection of lipid peroxidation. Scale bar: 200 μm. (P–R) The protein expression levels of GPX4 and 4-HNE were assessed using immunoblotting in TM3 cells. Data are shown as *mean* ± *S.E.M.* (n = 3–4 per group). $^{*}P < 0.05$, $^{**}P < 0.01$.

testes (Fig. 4C and D). Subsequently, it was found that Fer-1 effectively restored the environmental stress-downregulated the expression of the core antioxidant molecule GPX4, and reversed environmental stress-upregulated the expression of lipid peroxidation end product 4-HNE in mouse testes (Fig. 4E–G). Immunohistochemical analysis showed that 4-HNE was predominantly expressed in testicular Leydig cells, with pre-treatment by Fer-1 significantly reducing the accumulation of 4-HNE evoked by environmental stress (Fig. 4H and I). Interestingly, Fer-1 significantly restored the reduced levels of serum testosterone and the protein level of StAR and 3β-HSD in environmental stress-administered testes (Fig. 4J–M). Overall, environmental stress reduces testosterone levels by triggering ferroptosis in mouse testicular Leydig cells.

3.5. *Environmental stress upregulates Plin4 expression and induces lipid droplet deposition in mouse testicular Leydig cells*

To elucidate the mechanism of environmental stress-activated ferroptosis, the levels of lipid droplets were measured in mouse testes. As shown in Fig. 5A and B, TEM results revealed that environmental stress increased the accumulation of lipid droplets in testicular Leydig cells.

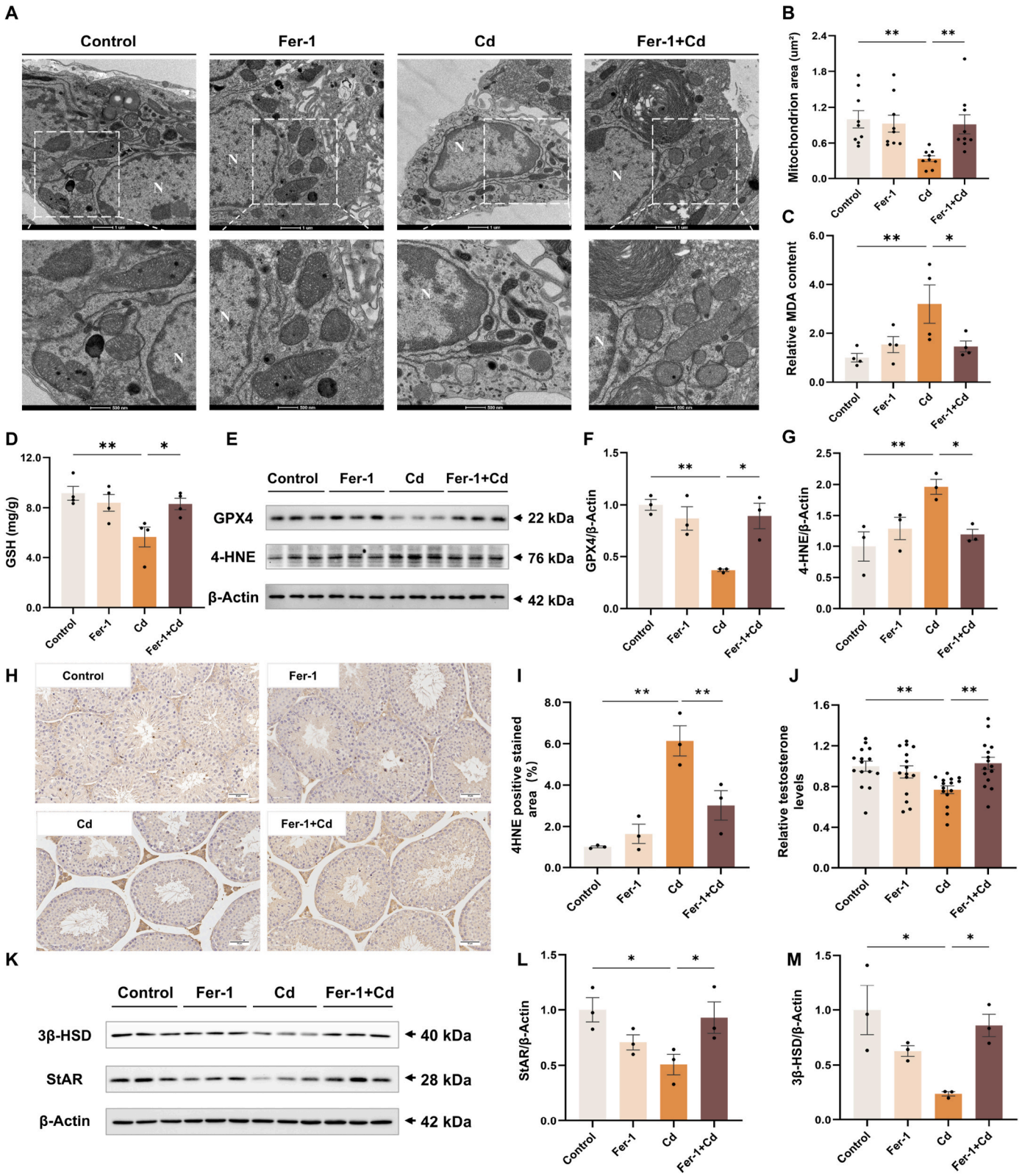

Fig. 4. Environmental stress reduces testosterone levels by inducing ferroptosis in mouse testicular Leydig cells. All male mice were intraperitoneally injected with 2 mg/kg ferrostatin-1, and 30 min later, 1 mg/kg $CdCl_2$ was injected once daily for three days. Mouse sera and testes were collected. (A) Representative transmission electron microscopy (TEM) images and their magnified images of mouse testicular Leydig cells. (B) Mitochondrial area for TEM images. (C) Malondialdehyde (MDA) content in testes. (D) Glutathione content in testes. (E–G) The protein expression levels of GPX4 and 4-HNE were assessed using immunoblotting in mouse testes. (H and I) Immunohistochemical detection of 4-HNE positive areas in the testes. (J) Serum testosterone levels. (K–M) The protein expression levels of 3β-HSD and StAR were evaluated using immunoblotting in mouse testes. Data are shown as *mean* ± *S.E.M.* (n = 3–15 per group). $^{*}P < 0.05$, $^{**}P < 0.01$.

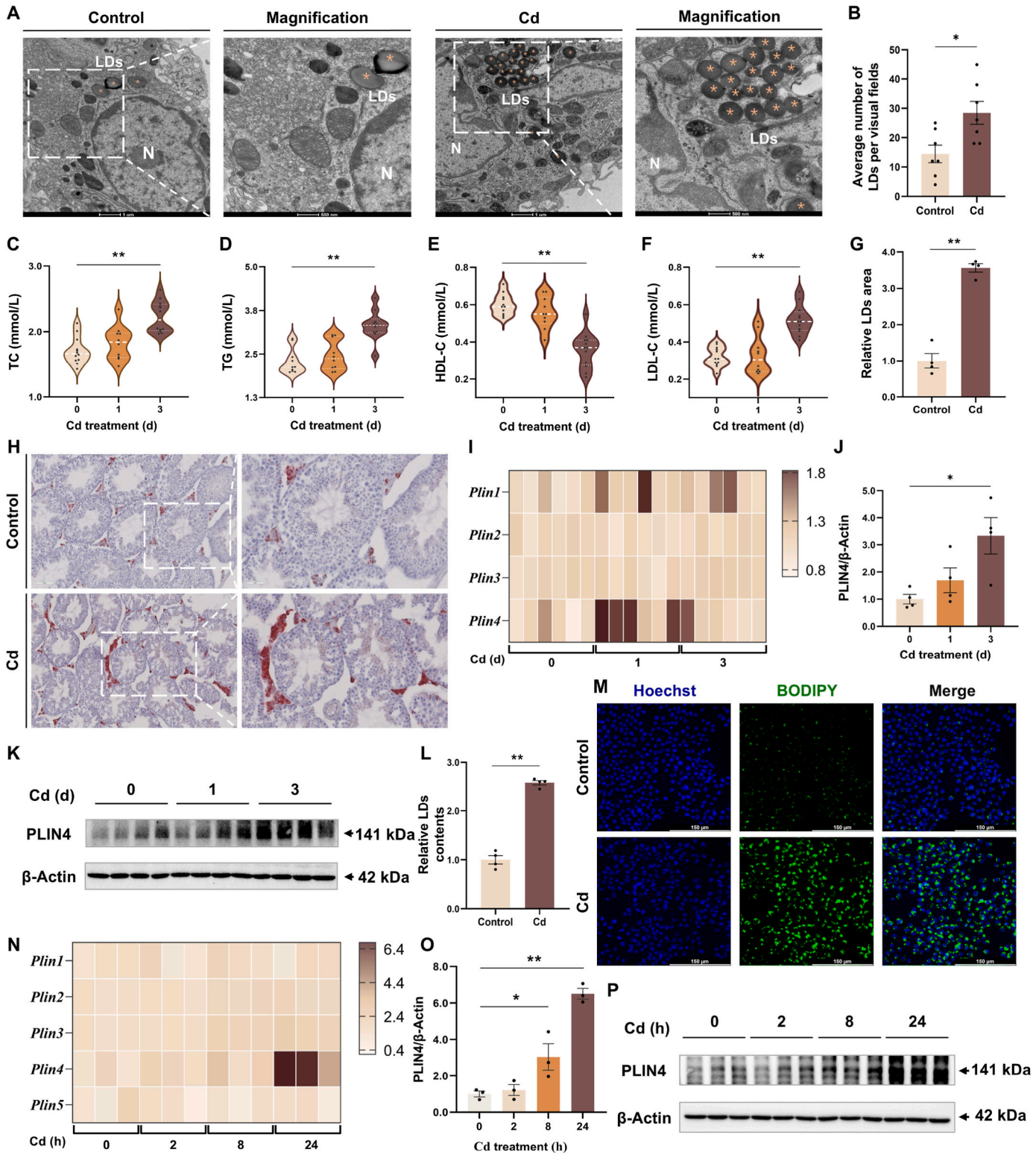

Fig. 5. Environmental stress upregulates *Plin4* expression and induces lipid droplets deposition in mouse testicular Leydig cells. (A–K) Male mice received an intraperitoneal injection of 1 mg/kg $CdCl_2$ daily for three days. Mouse sera and testes were collected. (A) Representative transmission electron microscopy (TEM) images and their magnified images of mouse testicular Leydig cells. (B) Quantitative results of lipid droplets (LDs) in TEM images. (C) Total cholesterol (TC) in serum. (D) Triglycerides (TG) in serum. (E) HDL cholesterol (HDL-C) in serum. (F) LDL cholesterol (LDL-C) in serum. (G and H) Quantitative results of oil red O staining and LDs area ratio in testes. Scale bar: 100 μm. (I) Heatmap of RT-qPCR detection of *Plin1*, *Plin2*, *Plin3*, and *Plin4* mRNA levels in the testes. (J and K) The protein expression levels of PLIN4 were assessed using immunoblotting in mouse testes. (L–P) Mouse testicular Leydig cells (TM3) were exposed to $CdCl_2$ (20 μM) for 0–24 h. (L and M) Representative images and quantitative results of BODIPY staining for the number of LDs in TM3 cells. Scale bar: 150 μm. (N) Heatmap of RT-qPCR analysis of *Plin1*, *Plin2*, *Plin3*, *Plin4* and *Plin5* mRNA levels in TM3 cells. (O and P) The protein expression levels of PLIN4 were evaluated using immunoblotting in TM3 cells. Data are shown as *mean* ± *S.E.M.* (n = 3–10 per group). $^{*}P < 0.05$, $^{**}P < 0.01$. (For interpretation of the references to color in this figure legend, the reader is referred to the Web version of this article.)

Environmental stress significantly increased TG, TC, and LDL-C levels, and notably decreased HDL-C levels in mouse sera, which was similar to the findings in populations with testosterone deficiency (Fig. 5C–F). Additionally, oil red O staining results showed that environmental stress led to considerable deposition of lipid droplets in testicular Leydig cells (Fig. 5G and H). To thoroughly investigate the causes of lipid droplet deposition upon environmental stress, RT-qPCR was utilized to screen the gene expression levels involved in lipid droplets formation. We found that environmental stress notably enhanced *Plin4* mRNA levels (Fig. 5I). In line, the PLIN4 protein was also elevated in environmental stress-exposed testes (Fig. 5J and K). To further delineate the circumstances of lipid droplet deposition, we conducted detailed analyses of testicular Leydig cells (TM3). Our data also showed that environmental stress significantly elevated the number of BODIPY-stained LDs in TM3 cells (Fig. 5L and M). Correspondingly, environmental stress markedly elevated mRNA and protein levels of PLIN4 in TM3 cells (Fig. 5N–P). The aforementioned results indicate that environmental stress upregulates the expression of *Plin4* and induces lipid droplet deposition in mouse

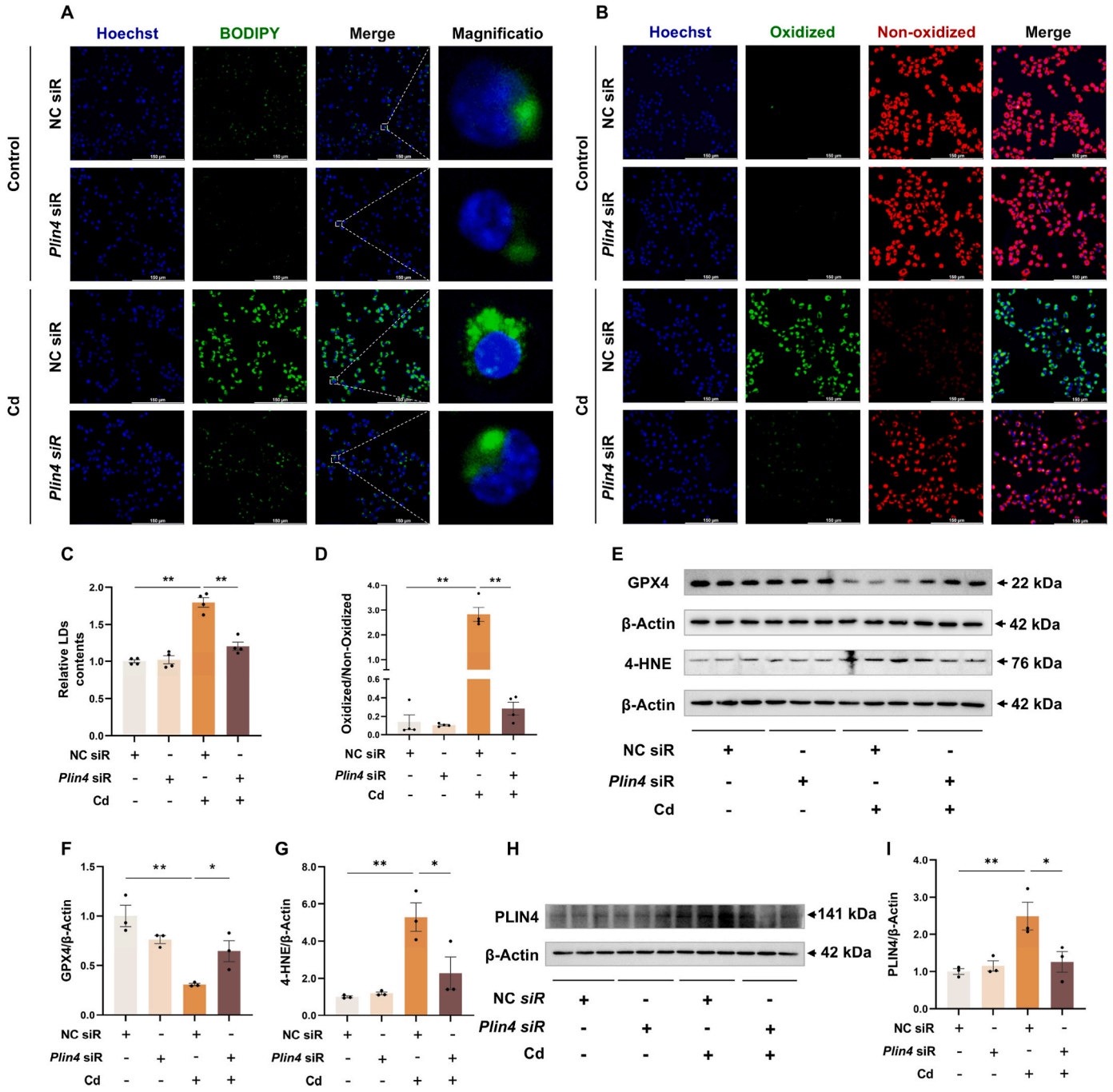

Fig. 6. Environmental stress induces ferroptosis via enhancing *Plin4*-mediated lipid droplet deposition in mouse testicular Leydig cells. TM3 cells were exposed with $CdCl_2$ (20 μM) for 0–24 h, with or without *Plin4* siR. (A–D) In TM3 cells, BODIPY fluorescence staining was used to detect the number of lipid droplets, while C11-BODIPY fluorescence staining was employed for lipid peroxidation detection. (A) Exemplary images of BODIPY fluorescence staining. Scale bar: 150 μm. (B) Exemplary images of C11-BODIPY fluorescence staining. Scale bar: 150 μm. (C) Quantitative results of lipid droplets (LDs). (D) Quantification for lipid peroxidation. (E–G) The protein expression levels of GPX4 and 4-HNE were assessed using immunoblotting. (H and I) The protein expression levels of PLIN4 were evaluated using immunoblotting. Data are shown as *mean* ± *S.E.M.* (n = 3–4 per group). $^{*}P < 0.05$, $^{**}P < 0.01$.

testicular Leydig cells.

3.6. Environmental stress induces ferroptosis via enhancing Plin4-mediated lipid droplet deposition in mouse testicular Leydig cells

To explore whether environmental stress induces ferroptosis by elevating *Plin4*-mediated lipid droplet deposition in Leydig cells, TM3 cells were pretreated with *Plin4* siRNA (siR) prior to treatment with the environmental stressor. As shown in Fig. 6A–D, *Plin4* siR treatment reduced the accumulation of lipid droplets and elevation of lipid peroxidation levels induced by environmental stress. Correspondingly, significant downregulation of PLIN4 and 4-HNE and upregulation of GPX4 were observed in TM3 cells pretreated with *Plin4* siR upon environmental stress (Fig. 6E–I). Interestingly, *Plin4* siR treatment significantly restored the reduced levels of cell medium testosterone and the protein level of StAR and 3β-HSD in environmental stress-administered TM3 cells (Figs. S5A–D). Overall, environmental stress induces ferroptosis via enhancing *Plin4*-mediated lipid droplet deposition in mouse testicular Leydig cells.

3.7. S-adenosylhomocysteine (SAH) supplementation alleviates environmental stress-elevated Plin4 and Fe^{2+} levels in mouse testicular Leydig cells

To investigate the mechanism of *Plin4* expression upregulated via environmental stress, the m6A modification level was measured in mouse testicular Leydig cells (TM3). Our findings showed that environmental stress significantly elevated the total RNA m6A modification levels (Fig. 7A). Additionally, environmental stress increased the protein levels of METTL3 and METTL14 (the m6A methyltransferase complex) (Fig. 7B–D). Furthermore, the MELLT3-METTL14 heterodimer complex activity inhibitor S-adenosylhomocysteine (SAH) was used to investigate the effects of m6A modification on *Plin4* upregulation and ferroptosis in environmental stress-exposed TM3 cells. Our data showed that SAH intervention reversed the significant increase in m6A modifications in total RNA induced by environmental stress. (Fig. 7E). Additionally, SAH intervention significantly alleviated the upregulation of PLIN4 by environmental stress (Fig. 7F and G). Concurrently, immunofluorescence and BODIPY staining revealed that SAH intervention markedly alleviated environmental stress-induced elevation of PLIN4 levels and accumulation of lipid droplets (Fig. 7H–J). Crucially, SAH intervention reversed the increase in ferrous iron (Fe^{2+}) levels and restored the decreased testosterone levels induced by environmental stress. (Fig. 7K and M). Thus, SAH supplementation alleviates environmental stress-increased *Plin4* and Fe^{2+} levels in mouse testicular Leydig cells.

4. Discussion

Testosterone, a male hormone primarily produced by the testes, is essential for the development of male sexual characteristics, spermatogenesis and reproductive function [53,54]. Testosterone deficiency (TD) is a significant global medical issue, affecting 30 % of men aged 40 to 79 [55,56]. As testosterone levels gradually decrease, patients with TD experience psychological, physiological, and metabolic effects that lower their quality of life [57]. Increasing research indicates that environmental factors are the primary cause of the gradual decline in testosterone levels [58]. Cadmium (Cd), a widely distributed heavy metal, is a common environmental stressor that induces reproductive toxicity [59–61]. This study demonstrated that environmental stress significantly downregulated key testosterone synthases expression, and reduced testosterone levels in vivo and in vitro. These findings were consistent with earlier research, which found that Cd significantly lowered testosterone levels in male mice [16,62,63]. Thus, environmental stress leads to a decrease in testosterone levels.

In the present study, our male reproductive cohort found that testosterone levels were negatively correlated with ferrous iron (Fe^{2+}) levels. Ferroptosis is a form of cell death dependent on the accumulation of Fe^{2+}, where Fe^{2+} catalyzes the Fenton reaction (Fe^{2+} reacting with hydrogen peroxide to produce hydroxyl radicals), promoting lipid peroxidation, and thereby leading to the depletion of the cellular antioxidant system [64–68]. The significance of ferroptosis in male reproductive injury has been established, particularly its crucial role in regulating testicular development, spermatogenesis, and blood-testis barrier (BTB) function [28,69–71]. Our results showed that environmental stress led to Fe^{2+} accumulation, increased lipid peroxidation levels, and decreased levels of glutathione (GSH) and GPX4 in testicular Leydig cells. The above results indicate that environmental stress triggers ferroptosis in testicular Leydig cells. Further experiments demonstrated that pretreatment with ferrostatin-1 (Fer-1, the ferroptosis-specific inhibitor) restored environmental stress-reduced testosterone levels in mice. Therefore, our findings suggest that environmental stress lowers testosterone levels by inducing ferroptosis in mouse testicular Leydig cells.

Lipid droplets, the dynamic lipid storage organelles, play a crucial role in lipid homeostasis and testicular spermatogenesis [38,72,73]. Moreover, excessive lipid droplets possibly promote ferroptosis through the excessive oxidation of lipids [74]. Our research presented that environmental stress significantly elevated the number of oil red O and BODIPY-stained lipid droplets in testicular Leydig cells. It is widely recognized that lipid droplets are consist of a surface phospholipid monolayer and specific proteins [36,75]. Among these proteins, the perilipin family has been noted for its functions of stabilizing lipid droplet's structure and regulating lipid storage [41]. In this study, we screened and identified the upregulated expression of *Plin4* in environmental stress-exposed testes. Subsequently, *Plin4* siR reversed environmental stress-induced lipid droplet deposition and reduced the occurrence of ferroptosis in testicular Leydig cells. An earlier study discovered *Plin4*-dependent lipid droplet accumulation in neurons, which could be also reversed by *Plin4* siR intervention [45]. Thus, Environmental stress induces ferroptosis via enhancing *Plin4*-mediated lipid droplet deposition in mouse testicular Leydig cells.

*N*6-methyladenosine (m6A) is the most common RNA modification in eukaryotes, playing crucial roles in pathological and physiological processes [76,77]. m6A modification participates in many important physiological processes such as lipid metabolism and lipid droplet synthesis in mammals [78,79]. In this study, we found that environmental stress increased the total RNA m6A levels in mouse testicular Leydig cells, accompanied by a significant upregulation of key RNA methyltransferases METTL3 and METTL14. Previous studies have shown that S-adenosylhomocysteine (SAH), an activity inhibitor of the METTL3 and METTL14 heterodimer, could significantly decrease total m6A levels [80,81]. Our findings showed that SAH supplementation alleviated the environmental stress-induced upregulation of *Plin4* expression and accumulation of lipid droplets, and reversed environmental stress-increased the level of Fe^{2+} in mouse testicular Leydig cells. Similarly, a recent study also indicated that inhibiting the increase in m6A levels can effectively mitigate the occurrence of ferroptosis induced by another environmental stress [82]. As mentioned above, environmental stress upregulates *Plin4* in an m6A-dependent manner in mouse testicular Leydig cells.

5. Conclusion

In the current study, we observed the negative correlation between testosterone levels and Fe^{2+} levels in our male reproductive cohort. Through Fer-1 intervention experiments, we confirmed that ferroptosis contributes to the decline in testosterone levels caused by environmental stress. Additionally, we verified that environmental stress triggers ferroptosis by enhancing *Plin4*-mediated lipid droplet deposition, using *Plin4* siR. Finally, we used SAH to confirm that environmental stress upregulates *Plin4* in an m6A-dependent manner. In conclusion, *Plin4* exacerbates environmental stress-decreased testosterone level via

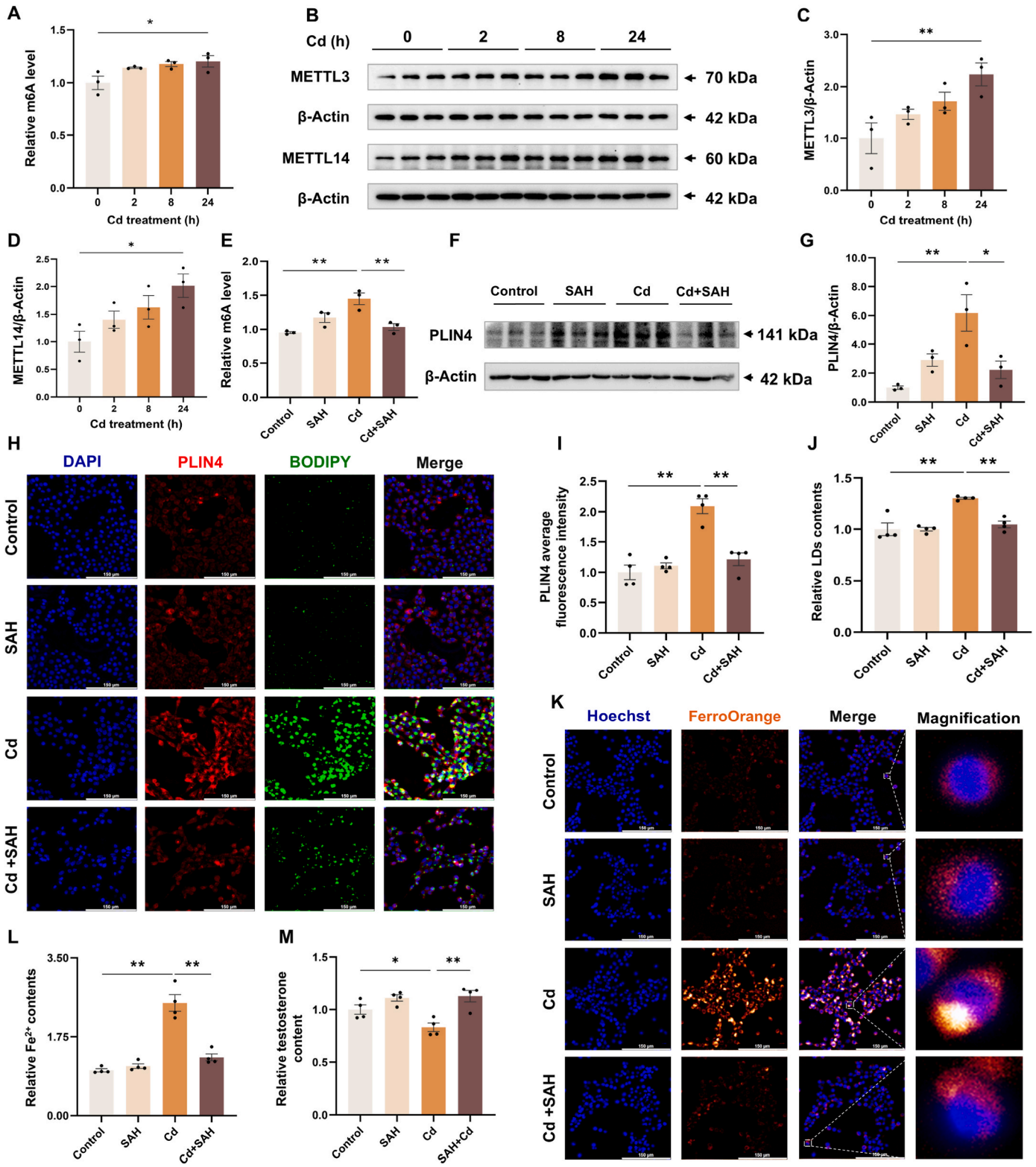

Fig. 7. S-adenosylhomocysteine (SAH) supplementation alleviates environmental stress-increased *Plin4* and Fe^{2+} levels in mouse testicular Leydig cells. (A–D) Mouse testicular Leydig cells (TM3) were exposed to $CdCl_2$ (20 μM) for 0–24 h. (A) The total RNA m6A levels. (B–D) The protein expression levels of METTL3 and METTL14 were assessed using immunoblotting. (E–K) TM3 cells were treated with $CdCl_2$ (20 μM) for 24 h, with or without 10 μM S-adenosylhomocysteine (SAH). (E) Measurement of total RNA m6A levels. (F and G) The protein expression levels of PLIN4 were assessed using immunoblotting. (H–J) Exemplary immunofluorescence staining images and quantitative results of PLIN4 and lipid droplets, with nuclei marked by DAPI. Scale bar: 150 μm. (K and L) Exemplary images of FerroOrange fluorescence staining and quantitative results of ferrous iron (Fe^{2+}), with nuclei marked by Hoechst 33342. Scale bar: 150 μm. (M) Testosterone levels in cell media. Data are shown as *mean* ± *S.E.M.* (n = 3–4 per group). $^{*}P < 0.05$, $^{**}P < 0.01$.

inducing ferroptosis in testicular Leydig cells. *Plin4* may serve as a potential target for developing new drugs to treat testosterone deficiency and related reproductive disorders.

Consent for publication

The graphical abstract and flowchart was created using BioRender. We have obtained the necessary license (JD26ZLEBN6 and TW26ZLESD8) to use content from BioRender.

Funding

This work was supported by Center for Big Data and Population Health of IHM (JKS2022016), National Key Research and Development Program of China (2022YFC2702904), National Natural Science Foundation of China (82273664), and the Anhui Medical University Foundation Project (2023xkj008).

CRediT authorship contribution statement

Xu-Dong Zhang: Writing – original draft, Formal analysis, Data curation, Conceptualization. **Jian Sun:** Resources, Data curation. **Xin-Mei Zheng:** Formal analysis. **Jin Zhang:** Methodology. **Lu-Lu Tan:** Methodology. **Long-Long Fan:** Data curation. **Ye-Xin Luo:** Data curation. **Yi-Fan Hu:** Resources. **Shen-Dong Xu:** Investigation. **Huan Zhou:** Investigation. **Yu-Feng Zhang:** Methodology. **Hao Li:** Methodology. **Zhi Yuan:** Methodology. **Tian Wei:** Supervision. **Hua-Long Zhu:** Supervision. **De-Xiang Xu:** Supervision. **Yong-Wei Xiong:** Writing – review & editing, Conceptualization. **Hua Wang:** Writing – review & editing, Funding acquisition, Conceptualization.

Declaration of competing interest

The authors declare that they have no known competing financial interests or personal relationships that could have appeared to influence the work reported in this paper.

Data availability

Data will be made available on request.

Acknowledgements

We extend our sincere thanks to the Center for Scientific Research of Anhui Medical University and to our laboratory colleagues for their invaluable support throughout our experiment. We also greatly appreciate Dr. Xiao-Jin He and Dr. Hao Geng from the Reproductive Center of the First Affiliated Hospital of Anhui Medical University for their assistance in recruiting clinical participants.

Appendix A. Supplementary data

Supplementary data to this article can be found online at https://doi.org/10.1016/j.redox.2024.103312.

References

[1] G. Hackett, M. Kirby, D. Edwards, T.H. Jones, J. Rees, A. Muneer, UK policy statements on testosterone deficiency, Int. J. Clin. Pract. 71 (2017).
[2] J.D. Dean, C.G. McMahon, A.T. Guay, A. Morgentaler, S.E. Althof, E.F. Becher, et al., The isociety for sexual medicine's process of care for the assessment and management of testosterone deficiency in adult men, J. Sex. Med. 12 (2015) 1660–1686.
[3] M. Khera, G. Adaikan, J. Buvat, S. Carrier, A. El-Meliegy, K. Hatzimouratidis, et al., Diagnosis and treatment of testosterone deficiency: recommendations from the fourth international consultation for sexual medicine (ICSM 2015), J. Sex. Med. 13 (2016) 1787–1804.
[4] T. Mulligan, M.F. Frick, Q.C. Zuraw, A. Stemhagen, C. McWhirter, Prevalence of hypogonadism in males aged at least 45 years: the HIM study, Int. J. Clin. Pract. 60 (2006) 762–769.
[5] A. Tajar, G. Forti, T.W. O'Neill, D.M. Lee, A.J. Silman, J.D. Finn, et al., Characteristics of secondary, primary, and compensated hypogonadism in aging men: evidence from the European Male Ageing Study, J. Clin. Endocrinol. Metabol. 95 (2010) 1810–1818.
[6] S.J. Zhou, M.J. Zhao, Y.H. Yang, D. Guan, Z.G. Li, Y.D. Ji, et al., The epidemiological characteristics of late-onset hypogonadism in Chinese middle-aged and elderly men: two cross-sectional studies in the same community, Am. J. Men's Health 14 (2020) 1557988320977991.
[7] C. Chang, Y.T. Chen, S.D. Yeh, Q. Xu, R.S. Wang, F. Guillou, et al., Infertility with defective spermatogenesis and hypotestosteronemia in male mice lacking the androgen receptor in Sertoli cells, Proc. Natl. Acad. Sci. U.S.A. 101 (2004) 6876–6881.
[8] N.E. Skakkebaek, E. Rajpert-De Meyts, G.M. Buck Louis, J. Toppari, A. M. Andersson, M.L. Eisenberg, et al., Male reproductive disorders and fertility trends: influences of environment and genetic susceptibility, Physiol. Rev. 96 (2016) 55–97.
[9] F. Lotti, M. Maggi, Sexual dysfunction and male infertility, Nat. Rev. Urol. 15 (2018) 287–307.
[10] A.M. Andersson, N. Jørgensen, L. Frydelund-Larsen, E. Rajpert-De Meyts, N. E. Skakkebaek, Impaired Leydig cell function in infertile men: a study of 357 idiopathic infertile men and 318 proven fertile controls, J. Clin. Endocrinol. Metabol. 89 (2004) 3161–3167.
[11] I.A. Olesen, U.N. Joensen, J.H. Petersen, K. Almstrup, E. Rajpert-De Meyts, E. Carlsen, et al., Decrease in semen quality and Leydig cell function in infertile men: a longitudinal study, Hum. Reprod. 33 (2018) 1963–1974.
[12] G. Grande, F. Barrachina, A. Soler-Ventura, M. Jodar, F. Mancini, R. Marana, et al., The role of testosterone in spermatogenesis: lessons from proteome profiling of human spermatozoa in testosterone deficiency, Front. Endocrinol. 13 (2022) 852661.
[13] E.V. Munari, M. Amer, A. Amodeo, R. Bollino, S. Federici, G. Goggi, et al., The complications of male hypogonadism: is it just a matter of low testosterone? Front. Endocrinol. 14 (2023) 1201313.
[14] N. Dehdari Ebrahimi, S. Parsa, F. Nozari, M.A. Shahlaee, A. Maktabi, M. Sayadi, et al., Protective effects of melatonin against the toxic effects of environmental pollutants and heavy metals on testicular tissue: a systematic review and meta-analysis of animal studies, Front. Endocrinol. 14 (2023) 1119553.
[15] L. XueXia, L. YaNan, T. Zi, Z. YuSheng, W. ZeLin, Z. Peng, et al., Di-2-ethylhexyl phthalate (DEHP) exposure induces sperm quality and functional defects in mice, Chemosphere 312 (2023) 137216.
[16] T.T. Wang, H.L. Zhu, K.W. Ouyang, H. Wang, Y.X. Luo, X.M. Zheng, et al., Environmental cadmium inhibits testicular testosterone synthesis via Parkin-dependent MFN1 degradation, J. Hazard Mater. 470 (2024) 134142.
[17] T.G. Travison, A.B. Araujo, A.B. O'Donnell, V. Kupelian, J.B. McKinlay, A population-level decline in serum testosterone levels in American men, J. Clin. Endocrinol. Metabol. 92 (2007) 196–202.
[18] S. Roychoudhury, S. Chakraborty, A.P. Choudhury, A. Das, N.K. Jha, P. Slama, et al., Environmental factors-induced oxidative stress: hormonal and molecular pathway disruptions in hypogonadism and erectile dysfunction, Antioxidants 10 (2021). Basel, Switzerland.
[19] C. Chen, N. Wang, X. Nie, B. Han, Q. Li, Y. Chen, et al., Blood cadmium level associates with lower testosterone and sex hormone-binding globulin in Chinese men: from SPECT-China study, 2014, Biol. Trace Elem. Res. 171 (2016) 71–78.
[20] X. Zeng, T. Jin, J.P. Buchet, X. Jiang, Q. Kong, T. Ye, et al., Impact of cadmium exposure on male sex hormones: a population-based study in China, Environ. Res. 96 (2004) 338–344.
[21] J. Zhou, L. Zeng, Y. Zhang, M. Wang, Y. Li, Y. Jia, et al., Cadmium exposure induces pyroptosis in testicular tissue by increasing oxidative stress and activating the AIM2 inflammasome pathway, Sci. Total Environ. 847 (2022) 157500.
[22] M. Venditti, M. Ben Rhouma, M.Z. Romano, I. Messaoudi, R.J. Reiter, S. Minucci, Evidence of melatonin ameliorative effects on the blood-testis barrier and sperm quality alterations induced by cadmium in the rat testis, Ecotoxicol. Environ. Saf. 226 (2021) 112878.
[23] B.R. Stockwell, Ferroptosis turns 10: emerging mechanisms, physiological functions, and therapeutic applications, Cell 185 (2022) 2401–2421.
[24] S.J. Dixon, K.M. Lemberg, M.R. Lamprecht, R. Skouta, E.M. Zaitsev, C.E. Gleason, et al., Ferroptosis: an iron-dependent form of nonapoptotic cell death, Cell 149 (2012) 1060–1072.
[25] X. Jiang, B.R. Stockwell, M. Conrad, Ferroptosis: mechanisms, biology and role in disease, Nat. Rev. Mol. Cell Biol. 22 (2021) 266–282.
[26] Y. Liu, Y. Wan, Y. Jiang, L. Zhang, W. Cheng, GPX4: the hub of lipid oxidation, ferroptosis, disease and treatment, Biochim. Biophys. Acta Rev. Canc 1878 (2023) 188890.
[27] K. Wu, M. Yan, T. Liu, Z. Wang, Y. Duan, Y. Xia, et al., Creatine kinase B suppresses ferroptosis by phosphorylating GPX4 through a moonlighting function, Nat. Cell Biol. 25 (2023) 714–725.
[28] Y.Q. Feng, X. Liu, N. Zuo, M.B. Yu, W.M. Bian, B.Q. Han, et al., NAD(+) precursors promote the restoration of spermatogenesis in busulfan-treated mice through inhibiting Sirt2-regulated ferroptosis, Theranostics 14 (2024) 2622–2636.
[29] X. Liu, Y. Ai, M. Xiao, C. Wang, Z. Shu, J. Yin, et al., PM 2.5 juvenile exposure-induced spermatogenesis dysfunction by triggering testes ferroptosis and antioxidative vitamins intervention in adult male rats, Environ. Sci. Pollut. Res. Int. 30 (2023) 111051–111061.

[30] Z. Zhang, J. Cheng, L. Yang, X. Li, R. Hua, D. Xu, et al., The role of ferroptosis mediated by Bmal1/Nrf 2 in nicotine -induce injury of BTB integrity, Free Radic. Biol. Med. 200 (2023) 26–35.
[31] Y. Wang, J. Wu, M. Zhang, H. OuYang, M. Li, D. Jia, et al., Cadmium exposure during puberty damages testicular development and spermatogenesis via ferroptosis caused by intracellular iron overload and oxidative stress in mice, Environ. Pollut. 325 (2023) 121434.
[32] Y.Y. Guo, N.N. Liang, X.Y. Zhang, Y.H. Ren, W.Z. Wu, Z.B. Liu, et al., Mitochondrial GPX4 acetylation is involved in cadmium-induced renal cell ferroptosis, Redox Biol. 73 (2024) 103179.
[33] L. Wang, X. Zhang, M. Xu, G. Zheng, J. Chen, S. Li, et al., Implication of ferroptosis in hepatic toxicity upon single or combined exposure to polystyrene microplastics and cadmium, Environ. Pollut. 334 (2023) 122250.
[34] H. Hong, X. Lin, Y. Xu, T. Tong, J. Zhang, H. He, et al., Cadmium induces ferroptosis mediated inflammation by activating Gpx4/Ager/p65 axis in pancreatic β-cells, Sci. Total Environ. 849 (2022) 157819.
[35] T. Zhang, W. Yan, C. Liu, W. Duan, Y. Duan, Y. Li, et al., Cadmium exposure promotes ferroptosis by upregulating Heat Shock Protein 70 in vascular endothelial damage of zebrafish, Ecotoxicol. Environ. Saf. 263 (2023) 115241.
[36] J.A. Olzmann, P. Carvalho, Dynamics and functions of lipid droplets, Nat. Rev. Mol. Cell Biol. 20 (2019) 137–155.
[37] A. Zadoorian, X. Du, H. Yang, Lipid droplet biogenesis and functions in health and disease, Nat. Rev. Endocrinol. 19 (2023) 443–459.
[38] C.F. Chao, Y.Y. Pesch, H. Yu, C. Wang, M.J. Aristizabal, T. Huan, et al., An important role for triglyceride in regulating spermatogenesis, Elife 12 (2024).
[39] J.J. Jiang, G.F. Zhang, J.Y. Zheng, J.H. Sun, S.B. Ding, Targeting mitochondrial ROS-mediated ferroptosis by quercetin alleviates high-fat diet-induced hepatic lipotoxicity, Front. Pharmacol. 13 (2022) 876550.
[40] C. Sztalryd, D.L. Brasaemle, The perilipin family of lipid droplet proteins: gatekeepers of intracellular lipolysis, Biochim. Biophys. Acta Mol. Cell Biol. Lipids 1862 (2017) 1221–1232.
[41] A.R. Kimmel, C. Sztalryd, The perilipins: major cytosolic lipid droplet-associated proteins and their roles in cellular lipid storage, mobilization, and systemic homeostasis, Annu. Rev. Nutr. 36 (2016) 471–509.
[42] M. Conte, C. Franceschi, M. Sandri, S. Salvioli, Perilipin 2 and age-related metabolic diseases: a new perspective, Trends Endocrinol. Metabol.: TEM (Trends Endocrinol. Metab.) 27 (2016) 893–903.
[43] J. Li, Q. Zhang, Y. Guan, D. Liao, H. Chen, H. Xiong, et al., TRIB3 promotes the progression of renal cell carcinoma by upregulating the lipid droplet-associated protein PLIN2, Cell Death Dis. 15 (2024) 240.
[44] W. Chen, B. Chang, X. Wu, L. Li, M. Sleeman, L. Chan, Inactivation of Plin4 downregulates Plin5 and reduces cardiac lipid accumulation in mice, Am. J. Physiol. Endocrinol. Metabol. 304 (2013) E770–E779.
[45] X. Han, J. Zhu, X. Zhang, Q. Song, J. Ding, M. Lu, et al., Plin4-Dependent lipid droplets hamper neuronal mitophagy in the MPTP/p-Induced mouse model of Parkinson's disease, Front. Neurosci. 12 (2018) 397.
[46] A.C. Martins, M.R. Urbano, A.C.B. Almeida Lopes, M.F.H. Carvalho, M.L. Buzzo, A. O. Docea, et al., Blood cadmium levels and sources of exposure in an adult urban population in southern Brazil, Environ. Res. 187 (2020) 109618.
[47] L. Zeng, J. Zhou, X. Wang, Y. Zhang, M. Wang, P. Su, Cadmium attenuates testosterone synthesis by promoting ferroptosis and blocking autophagosome-lysosome fusion, Free Radic. Biol. Med. 176 (2021) 176–188.
[48] Y.W. Xiong, X.F. Xu, H.L. Zhu, X.L. Cao, S.J. Yi, X.T. Shi, et al., Environmental exposure to cadmium impairs fetal growth and placental angiogenesis via GCN-2-mediated mitochondrial stress, J. Hazard Mater. 401 (2021) 123438.
[49] A. Mehlem, C.E. Hagberg, L. Muhl, U. Eriksson, A. Falkevall, Imaging of neutral lipids by oil red O for analyzing the metabolic status in health and disease, Nat. Protoc. 8 (2013) 1149–1154.
[50] Y.W. Xiong, H.L. Zhu, J. Zhang, H. Geng, L.L. Tan, X.M. Zheng, et al., Multigenerational paternal obesity enhances the susceptibility to male subfertility in offspring via Wt1 N6-methyladenosine modification, Nat. Commun. 15 (2024) 1353.
[51] Y.W. Xiong, L.L. Tan, J. Zhang, H.L. Zhu, X.M. Zheng, W. Chang, et al., Combination of high-fat diet and cadmium impairs testicular spermatogenesis in an m6A-YTHDF2-dependent manner, Environ. Pollut. 313 (2022) 120112.
[52] H.L. Zhu, X.T. Shi, X.F. Xu, G.X. Zhou, Y.W. Xiong, S.J. Yi, et al., Melatonin protects against environmental stress-induced fetal growth restriction via suppressing ROS-mediated GCN2/ATF4/BNIP3-dependent mitophagy in placental trophoblasts, Redox Biol. 40 (2021) 101854.
[53] L.B. Smith, W.H. Walker, The regulation of spermatogenesis by androgens, Semin. Cell Dev. Biol. 30 (2014) 2–13.
[54] K. Khodamoradi, K. Campbell, H. Arora, R. Ramasamy, Evaluation of androgen receptor markers in erectile dysfunction, Andrology 12 (2024) 599–605.
[55] A.M. Traish, M.M. Miner, A. Morgentaler, M. Zitzmann, Testosterone deficiency, Am. J. Med. 124 (2011) 578–587.
[56] A. Morales, C.C. Schulman, J. Tostain, C.W.W. F, Testosterone Deficiency Syndrome (TDS) needs to be named appropriately–the importance of accurate terminology, Eur. Urol. 50 (2006) 407–409.
[57] .
[58] W. Rodprasert, J. Toppari, H.E. Virtanen, Environmental toxicants and male fertility, Best Pract. Res. Clin. Obstet. Gynaecol. 86 (2023) 102298.
[59] J. Shi, D. Zhao, F. Ren, L. Huang, Spatiotemporal variation of soil heavy metals in China: the pollution status and risk assessment, Sci. Total Environ. 871 (2023) 161768.
[60] C.C. Wang, Q.C. Zhang, C.A. Yan, G.Y. Tang, M.Y. Zhang, L.Q. Ma, et al., Heavy metal(loid)s in agriculture soils, rice, and wheat across China: status assessment and spatiotemporal analysis, Sci. Total Environ. 882 (2023) 163361.
[61] E.W. Wong, C.Y. Cheng, Impacts of environmental toxicants on male reproductive dysfunction, Trends Pharmacol. Sci. 32 (2011) 290–299.
[62] Y. Li, Y. Zhang, R. Feng, P. Zheng, H. Huang, S. Zhou, et al., Cadmium induces testosterone synthesis disorder by testicular cell damage via TLR4/MAPK/NF-κB signaling pathway leading to reduced sexual behavior in piglets, Ecotoxicol. Environ. Saf. 233 (2022) 113345.
[63] Y.L. Ji, H. Wang, P. Liu, Q. Wang, X.F. Zhao, X.H. Meng, et al., Pubertal cadmium exposure impairs testicular development and spermatogenesis via disrupting testicular testosterone synthesis in adult mice, Reprod. Toxicol. 29 (2010) 176–183.
[64] Y. Su, B. Zhao, L. Zhou, Z. Zhang, Y. Shen, H. Lv, et al., Ferroptosis, a novel pharmacological mechanism of anti-cancer drugs, Cancer Lett. 483 (2020) 127–136.
[65] W.S. Yang, B.R. Stockwell, Ferroptosis: death by lipid peroxidation, Trends Cell Biol. 26 (2016) 165–176.
[66] D. Tang, X. Chen, R. Kang, G. Kroemer, Ferroptosis: molecular mechanisms and health implications, Cell Res. 31 (2021) 107–125.
[67] F. Ursini, M. Maiorino, Lipid peroxidation and ferroptosis: the role of GSH and GPx4, Free Radic. Biol. Med. 152 (2020) 175–185.
[68] X. Chen, J. Li, R. Kang, D.J. Klionsky, D. Tang, Ferroptosis: machinery and regulation, Autophagy 17 (2021) 2054–2081.
[69] A. Ghoochani, E.C. Hsu, M. Aslan, M.A. Rice, H.M. Nguyen, J.D. Brooks, et al., Ferroptosis inducers are a novel therapeutic approach for advanced prostate cancer, Cancer Res. 81 (2021) 1583–1594.
[70] Y. Zhao, H. Zhang, J.G. Cui, J.X. Wang, M.S. Chen, H.R. Wang, et al., Ferroptosis is critical for phthalates driving the blood-testis barrier dysfunction via targeting transferrin receptor, Redox Biol. 59 (2023) 102584.
[71] J. Cheng, L. Yang, Z. Zhang, D. Xu, R. Hua, H. Chen, et al., Diquat causes mouse testis injury through inducing heme oxygenase-1-mediated ferroptosis in spermatogonia, Ecotoxicol. Environ. Saf. 280 (2024) 116562.
[72] S.J. Dixon, J.A. Olzmann, The cell biology of ferroptosis, Nat. Rev. Mol. Cell Biol. 25 (2024) 424–442.
[73] W.J. Shen, S. Azhar, F.B. Kraemer, Lipid droplets and steroidogenic cells, Exp. Cell Res. 340 (2016) 209–214.
[74] S. Cho, S.J. Hong, S.H. Kang, Y. Park, S.K. Kim, Alpha-lipoic acid attenuates apoptosis and ferroptosis in cisplatin-induced ototoxicity via the reduction of intracellular lipid droplets, Int. J. Mol. Sci. 23 (2022).
[75] M.A. Welte, Expanding roles for lipid droplets, Curr. Biol. : Cailiao Baohu 25 (2015) R470–R481.
[76] L. Liu, H. Li, D. Hu, Y. Wang, W. Shao, J. Zhong, et al., Insights into N6-methyladenosine and programmed cell death in cancer, Mol. Cancer 21 (2022) 32.
[77] X. Jiang, B. Liu, Z. Nie, L. Duan, Q. Xiong, Z. Jin, et al., The role of m6A modification in the biological functions and diseases, Signal Transduct. Targeted Ther. 6 (2021) 74.
[78] Y. Yang, J. Cai, X. Yang, K. Wang, K. Sun, Z. Yang, et al., Dysregulated m6A modification promotes lipogenesis and development of non-alcoholic fatty liver disease and hepatocellular carcinoma, Mol. Ther. : the journal of the American Society of Gene Therapy 30 (2022) 2342–2353.
[79] Z. Yang, G.L. Yu, X. Zhu, T.H. Peng, Y.C. Lv, Critical roles of FTO-mediated mRNA m6A demethylation in regulating adipogenesis and lipid metabolism: implications in lipid metabolic disorders, Genes & diseases 9 (2022) 51–61.
[80] W. Ke, L. Zhang, X. Zhao, Z. Lu, p53 m(6)A modulation sensitizes hepatocellular carcinoma to apatinib through apoptosis, Apoptosis : an international journal on programmed cell death 27 (2022) 426–440.
[81] S. Yang, X. Zhou, Z. Jia, M. Zhang, M. Yuan, Y. Zhou, et al., Epigenetic regulatory mechanism of ADAMTS12 expression in osteoarthritis, Mol. Med. 29 (2023) 86. Cambridge, Mass.
[82] J. Feng, P. Zhang, K. Chen, P. Huang, X. Liang, J. Dong, et al., Soot nanoparticles promote ferroptosis in dopaminergic neurons via alteration of m6A RNA methylation in Parkinson's disease, J. Hazard Mater. 473 (2024) 134691.